Bone 49 (2011) 485–492

Contents lists available at ScienceDirect

Bone

journal homepage: www.elsevier.com/locate/bone

Spatiotemporal delivery of bone morphogenetic protein enhances functional repair of segmental bone defects

Yash M. Kolambkar [a,1], Joel D. Boerckel [b,1], Kenneth M. Dupont [b,1], Mehmet Bajin [c,1], Nathaniel Huebsch [d], David J. Mooney [d], Dietmar W. Hutmacher [e,2], Robert E. Guldberg [b,*]

[a] Department of Biomedical Engineering, Parker H. Petit Institute for Bioengineering and Bioscience, Georgia Institute of Technology, 315 Ferst Dr, Atlanta, GA 30332, USA
[b] School of Mechanical Engineering, Parker H. Petit Institute for Bioengineering and Bioscience, Georgia Institute of Technology, 315 Ferst Dr, Atlanta, GA 30332, USA
[c] Department of Chemistry & Biochemistry, Parker H. Petit Institute for Bioengineering and Bioscience, Georgia Institute of Technology, 315 Ferst Dr, Atlanta, GA 30332, USA
[d] School of Engineering and Applied Sciences, Wyss Institute of Biologically Inspired Engineering, Harvard University, 29 Oxford St., 319 Pierce Hall, USA
[e] Institute of Health and Biomedical Innovation, Queensland University of Technology, George W. Woodruff School of Mechanical Engineering, Georgia Institute of Technology, 60 Musk Avenue, Kelvin Grove QLD 4059, Australia

ARTICLE INFO

Article history:
Received 19 March 2011
Revised 8 May 2011
Accepted 10 May 2011
Available online 18 May 2011

Edited by Thomas Eihorn

Keywords:
Bone regeneration
Drug delivery
Bone morphogenetic protein
Collagen
Nanofiber mesh
Alginate

ABSTRACT

Osteogenic growth factors that promote endogenous repair mechanisms hold considerable potential for repairing challenging bone defects. The local delivery of one such growth factor, bone morphogenetic protein (BMP), has been successfully translated to clinical practice for spinal fusion and bone fractures. However, improvements are needed in the spatial and temporal control of BMP delivery to avoid the currently used supraphysiologic doses and the concomitant adverse effects. We have recently introduced a hybrid protein delivery system comprised of two parts: a perforated nanofibrous mesh that spatially confines the defect region and a functionalized alginate hydrogel that provides temporal growth factor release kinetics. Using this unique spatiotemporal delivery system, we previously demonstrated BMP-mediated functional restoration of challenging 8 mm femoral defects in a rat model. In this study, we compared the efficacy of the hybrid system in repairing segmental bone defects to that of the current clinical standard, collagen sponge, at the same dose of recombinant human BMP-2. In addition, we investigated the specific role of the nanofibrous mesh tube on bone regeneration. Our results indicate that the hybrid delivery system significantly increased bone regeneration and improved biomechanical function compared to collagen sponge delivery. Furthermore, we observed that presence of the nanofiber mesh tube was essential to promote maximal mineralized matrix synthesis, prevent extra-anatomical mineralization, and guide an integrated pattern of bone formation. Together, these results suggest that spatiotemporal strategies for osteogenic protein delivery may enhance clinical outcomes by improving localized protein retention.

Introduction

Large bone defects caused by trauma, tumor resection or disease present a significant clinical problem. Current treatments include autologous and allogeneic bone grafting, and more recently ceramic and composite substitutes for these. Autologous bone grafting remains the gold standard for bone healing because of the rich biologic environment it provides, but this treatment modality is limited by the amount of graft material available and donor site morbidity [1,2]. Structural allografts have been used as an alternative, but are unable to support revascularization and remodeling, and therefore are associated with a high rate of complications [3,4]. Bone graft substitutes made from ceramics or polymers suffer from limited bioactivity, and usually need to be supplemented with osteogenic cells or bone graft material [5]. These limitations of the current bone repair options have driven the search for alternative treatment options. One of the most promising classes of bone regeneration therapies is based on local delivery of growth factors such as bone morphogenetic protein (BMP), vascular endothelial growth factor (VEGF) and transforming growth factor β (TGF-β) [6–9]. These signaling molecules stimulate endogenous repair mechanisms by recruiting and programming the patient's own progenitor cells.

Of the various growth factors involved in bone formation, the role of BMPs has perhaps been studied the most extensively (for reviews, see [10,11]). BMPs are necessary for fetal tissue development as well as for fracture repair [6,12,13]. BMPs are present primarily in native bone tissue, and serve to attract progenitor cells to the defect site and promote their osteogenic differentiation [14]. In the last decade, two

* Corresponding author. Fax: +1 404 385 1397.
E-mail addresses: yashk@gatech.edu (Y.M. Kolambkar), joel.boerckel@gatech.edu (J.D. Boerckel), kennethmdupont@yahoo.com (K.M. Dupont), bajin.mehmet@gmail.com (M. Bajin), nhuebsch@fas.harvard.edu (N. Huebsch), mooneyd@seas.harvard.edu (D.J. Mooney), dietmar.hutmacher@qut.edu.au (D.W. Hutmacher), robert.guldberg@me.gatech.edu (R.E. Guldberg).
[1] Fax: +1 404 385 1397.
[2] Fax: +61 7 3138 6030.

8756-3282/$ – see front matter © 2011 Elsevier Inc. All rights reserved.
doi:10.1016/j.bone.2011.05.010

recombinant human bone morphogenetic proteins, rhBMP-2 and rhBMP-7, have been approved by regulatory bodies worldwide for spinal fusion, oral-maxillofacial applications and the treatment of certain fractures [7,15]. However, challenges remain due to the suboptimal delivery vehicles, poor spatiotemporal dosage control and short protein half-life, which has resulted in the need for supraphysiologic concentrations of rhBMPs [16–18]. Currently, rhBMPs are delivered in solution on purified type I collagen matrix. However, extremely high doses (~60 μM compared to the physiological BMP range of 1–30 nM) are required for obtaining a substantial healing response due to the disadvantages mentioned above [19]. The high doses have resulted in complications arising due to diffusion of the BMP away from the defect site [20–22], and the high cost associated with producing these large quantities limits the routine use of BMPs [23,24].

Due to the limitations of collagen-based delivery of BMP, numerous sustained delivery vehicles are being developed to improve protein pharmacokinetics *in vivo* [25–27]. In addition to the sustained release of the protein, its spatial distribution at the defect site is also important to maximize efficacy and minimize ectopic bone formation. In a previous study, we demonstrated that a delivery system that utilizes an electrospun nanofiber mesh tube and alginate hydrogel to provide spatiotemporal control over BMP release results in the functional repair of large bone defects [28]. In this system, a nanofiber mesh tube is used to encapsulate the bone defect and RGD-functionalized alginate hydrogel that contains BMP is injected inside the tube. The alginate provides sustained availability of the growth factor and supports cell infiltration into the defect space, while the nanofiber mesh is intended to retain the hydrogel and growth factor within the defect site and define the region of bone regeneration. This hybrid approach thus provides both spatial and the temporal control of the exogenously delivered protein for effective bone regeneration.

The purpose of this study was to compare the hybrid alginate/nanofiber mesh delivery system with the clinical standard of BMP delivery on an absorbable collagen sponge. In addition, the role of the nanofiber mesh tube as a spatial constraint was investigated. Our hypotheses were that BMP delivery within alginate hydrogel would enhance bone formation compared to collagen delivery, and the presence of the mesh tube would result in improved localization of the regenerated bone and improved restoration of biomechanical function. To test these hypotheses, we evaluated the morphological and biomechanical properties of the regenerated bone in a challenging rat segmental defect model.

Materials and methods

Nanofiber mesh tube fabrication

Nanofiber meshes were made by electrospinning and formed into cylindrical tubes as described previously [28]. Briefly, a 12% (w/v) solution of poly (ε-caprolactone) (PCL; Sigma-Aldrich, St. Louis, MO) was made by dissolving the polymer in a 90:10 volume ratio of hexafluoro-2-propanol (HFP):dimethylformamide (DMF) (Sigma-Aldrich). The following parameters were used during electrospinning-flow rate: 0.75 mL/h; voltage: 13 kV; collector distance: 17 cm; needle gauge: 22. Fibers were collected for 6 h to obtain nanofiber meshes having a thickness of approximately 300–400 μm. The nanofiber mesh morphology was characterized by analyzing images obtained by a Scanning Electron Microscope (SEM; Hitachi HTA, Pleasanton, CA). Perforations measuring 1 mm in diameter and spaced approximately 1.5 mm apart were made in rectangular 13×19 mm mesh samples using a biopsy punch (Miltex Inc., York, PA). The mesh samples were then wrapped around a steel mandrel and glued using UV glue (DYMAX Corporation, Torrington, CT) to form hollow tubular implants having a diameter of approximately 5 mm and a length of approximately 13 mm. The perforated mesh tubes were sterilized by ethanol evaporation, rinsed with excess phosphate-buffered saline (PBS; Mediatech Inc., Manassas, VA) and stored in αMEM (Invitrogen, Carlsbad, CA) until implantation.

Alginate hydrogel preparation

Medical grade sodium alginate, MVG (FMC Biopolymer, Philadelphia, PA), was irradiated with 5 Mrad dose of gamma irradiation, and covalently coupled with RGD-containing G_4RGDASSP peptide sequences (Peptides International, Kentucky, LA), as previously described [29,30]. Alginate hydrogels, at a concentration of 2% (w/v) and encapsulating 33.33 μg/mL rhBMP-2 (R&D Systems, Minneapolis, MN), were prepared in 1 mL syringes by crosslinking the alginate with calcium sulfate slurry at a ratio of 25:1 [28]. For one of the experimental groups, cylindrical plugs (∅5 mm; 9 mm length) of alginate hydrogel were made by allowing the gelation to occur in a custom-built mold. The hydrogels were stored at 4 °C overnight prior to implantation on the following day.

Surgical procedure

An established rat femoral segmental defect model [31] was employed to compare the efficacy of three different rhBMP-2 delivery strategies. Briefly, the femora of 13-week-old female Sasco Sprague–Dawley rats were stabilized with fixation plates, and bilateral 8 mm segmental defects were created in the mid-femoral diaphyses with an oscillating saw. A 5 μg dose of rhBMP-2 was delivered to each defect in one of three different ways (Fig. 1 and Table 1). In the first group (Col), a collagen sponge (∅5 mm; 9 mm length) was soaked with 150 μL of 33.33 μg/mL rhMBP-2 solution for 15 minutes and implanted in the defect. The collagen sponges were cut from a fibrous collagen sheet (average pore size 61.7 μm, 93.7% pore volume; Kensey Nash, Exton, PA) using a biopsy punch. Implants in the second group (Alg) consisted of a cylindrical plug (∅5 mm; 9 mm length) made from alginate hydrogel containing 5 μg rhBMP-2. In the third group (Alg + Mesh), a perforated nanofiber mesh tube was placed around the defect, and 150 μL of pre-gelled alginate containing rhBMP-2 (rhBMP-2 concentration: 33.33 μg/mL) was injected inside the tube through the perforations. The animals were allowed to move freely after surgery and were given subcutaneous injections of buprenorphine for the first 72 h to reduce pain. All surgical procedures were approved by

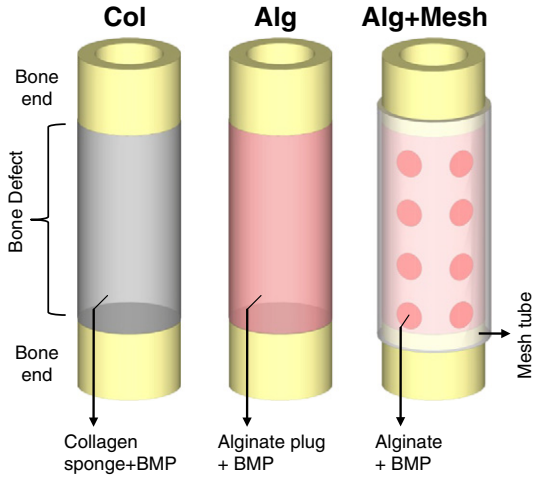

Fig. 1. Schematic representations of the three protein delivery strategies used in this study. The first group consisted of a collagen sponge soaked with rhMBP-2 and implanted in the defect (Col). The second group consisted of an alginate hydrogel plug with rhBMP-2 (Alg). In the third group, alginate hydrogel containing rhBMP-2 was injected inside a perforated nanofiber mesh tube placed at the defect (Alg + Mesh).

Table 1
Experimental groups utilized in the study.

Group	Designation	Description
I	Col	Collagen sponge + 5 μg rhBMP-2
II	Alg	Alginate plug + 5 μg rhBMP-2
III	Alg + Mesh	Alginate + Nanofiber mesh tube + 5 μg rhBMP-2

the Georgia Institute of Technology's Institutional Animal Care and Use Committee (IACUC; protocol #A08032).

Radiographic and μCT analysis

Radiographic and *in vivo* μCT evaluations of 8–10 samples per group were performed at 4 and 12 weeks following surgery to assess bone formation. Radiographs were also taken at 2 weeks to assess early differences between groups. The radiographs were taken with a Faxitron MX-20 Digital machine (Faxitron X-ray Corp., Wheeling, IL) using a voltage of 25 kV and an exposure time of 15 seconds. For the μCT imaging, the animals were anesthetized by isoflurane and placed in an *in vivo* μCT system (Viva-CT, Scanco Medical, Bassersdorf, Switzerland). The mid-femoral defect region was scanned using the following μCT parameters—voxel resolution: 38.5 μm; voltage: 55 kVp; current: 109 μA. The central 4 mm of the 8 mm defect was selected for the quantitative analysis for consistency between specimens. Two volumes of interest (VOI) were defined for the analysis of bone distribution. The central VOI was defined as the cylindrical volume that captured the central defect region within a diameter of 7 mm. The total VOI contained the entire volume of mineralization, in and around the defect, including any bone formation outside the defect region. Based on the two dimensional scan slices, an appropriate threshold was selected at each time point to detect bone while excluding soft tissues [28]. In addition to the volume of newly formed bone at each time point, μCT data was processed to obtain mean density, connectivity density and temporal changes in volume of the regenerated bone.

Biomechanical analysis

Following euthanasia of the animals at 12 weeks, torsional testing was performed on extracted femora to evaluate functional restoration of the limbs. The femora were cleaned of soft tissues and the ends potted in end blocks using Wood's metal (Alfa Aesar, Wood Hill, MA). After removal of the fixation plate, the specimens were tested on a Bose ElectroForce system (ELF 3200, Bose ElectroForce Systems Group, Minnetonka, MN) at a rotational rate of 3° per second. Maximum torque and failure angle were measured at the failure point from the torque-rotation data. Torsional stiffness was calculated by fitting a straight line to the linear portion of the curve before failure. Finally, work to failure was calculated by integrating the area under the torque-rotation curve up to the failure point.

Histological analysis

Histological analysis was performed at 12 weeks post-surgery on extracted femurs. The specimens were first fixed in 10% neutral buffered formalin for 48 h. After two brief rinses in deionized water, they were then decalcified in Cal-ExII (Fisher Scientific, Pittsburgh, PA) for 2 weeks under mild agitation. The decalcified femurs were dehydrated using a graded series of alcohol and embedded in a glycol methacrylate (GMA) formulation (Immuno-Bed, Polysciences Inc., Warrington, PA) using the manufacturer's instructions. Five micron-thick mid-sagittal sections were cut using a tungsten carbide blade on a rotary microtome, and the sections were stained with hematoxylin and eosin (H&E). Bright-field images were obtained with the Axio Observer.Z1 microscope (Carl Zeiss, Thornwood, NY). Images were taken at 4× and 10× magnification using the AxioVision software (Carl Zeiss). In addition, the low magnification images were stitched together using the same software to observe a larger region at the defect.

Data analysis

Data are presented as mean ± standard error of mean (SEM). Data were analyzed using analysis of variance (ANOVA) and Tukey's tests for pairwise comparisons (significance set at $p<0.05$). The normality of the data was verified by performing the Anderson–Darling test on residuals. When data were not normal, the nonparametric Mann–Whitney test was used to compare between groups. Minitab® 15 (Minitab Inc., State College, PA) was used for all statistical analysis.

Results

Radiographs

The radiographs of the defect region at the early time point of 2 weeks illustrated that a considerable amount of new bone was deposited in the group where rhBMP-2 was delivered on collagen sponge (Col) (Fig. 2). At the same time point, bone formation was also evident in the two alginate groups (Alg and Alg + Mesh), but the density appeared lower than in the collagen group. Conversely, the radiographs at 4 and 12 weeks suggested that the alginate groups exhibited higher amounts of de novo bone formation. It should be

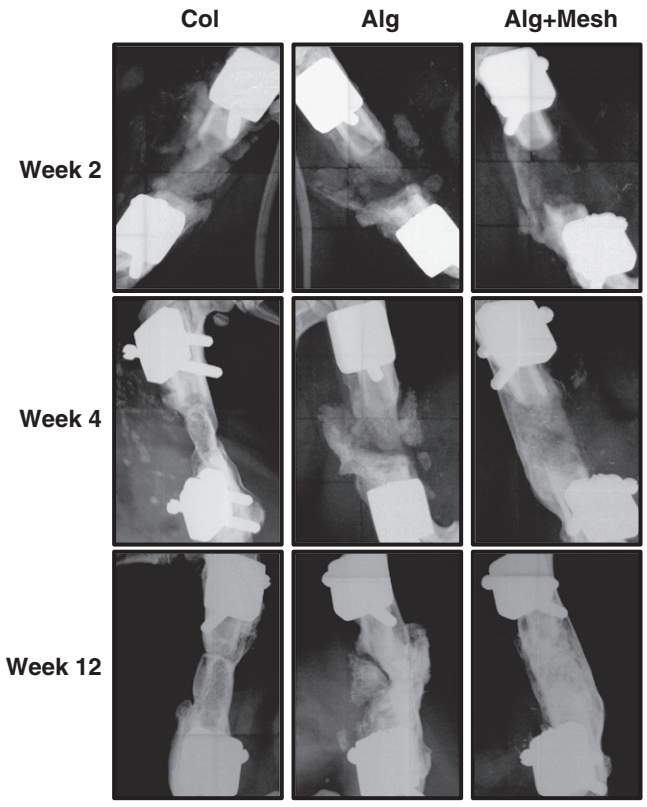

Fig. 2. Representative radiographs at 2, 4 and 12 weeks post-surgery. At 2 weeks, the Col specimens appeared to possess more bony tissue in the defect than the Alg and Alg + Mesh groups. However, at 4 and 12 weeks, defects in the two alginate groups demonstrated qualitatively higher bone formation. All defects in the three groups were bridged with bony tissue by 12 weeks. The newly formed bone in the alginate groups appeared more densely packed that that in the Col group. Note that the new bone formation was better contained within the defect in the Alg + Mesh group where the nanofiber mesh tube was present, compared to the Alg group. $n = 9–10$ defects per group.

noted that there was substantial bone regeneration in all groups at 4 weeks and bridging of all defects after 12 weeks. However, differences in the distribution and density of bone deposition were observed among groups. The Col group samples appeared to have more trabecular-like bone that was not as densely packed as the other two groups and there was an apparent contraction of the mineralization front to less than the diameter of the defect region. The Alg group demonstrated mineral deposition both within and outside the defect, suggesting some alginate hydrogel displacement or protein diffusion or combination of both. In contrast, samples in the Alg + Mesh group exhibited consistent localization of dense new bone formation inside the defect region.

μCT analysis

Three-dimensional μCT images obtained *in vivo* at 4 and 12 weeks were consistent with the radiographs (Fig. 3). The collagen sponge group (Col) possessed abundant new bone formation in the defects by 4 weeks. Specimens in the alginate scaffold group (Alg) exhibited a fragmented distribution of mineralized tissue, with substantial bone formation occurring outside the defect region. In contrast, in the presence of a nanofiber mesh tube (Alg + Mesh), new bone formation was confined within the defect region and displayed a continuous distribution.

Quantitative μCT analysis demonstrated that the amount and distribution of regenerated bone was significantly affected by the rhBMP-2 delivery method. At 4 weeks, the alginate delivery groups (Alg and Alg + Mesh) had significantly more total bone formation than the collagen delivery group (Col) and the trends were similar

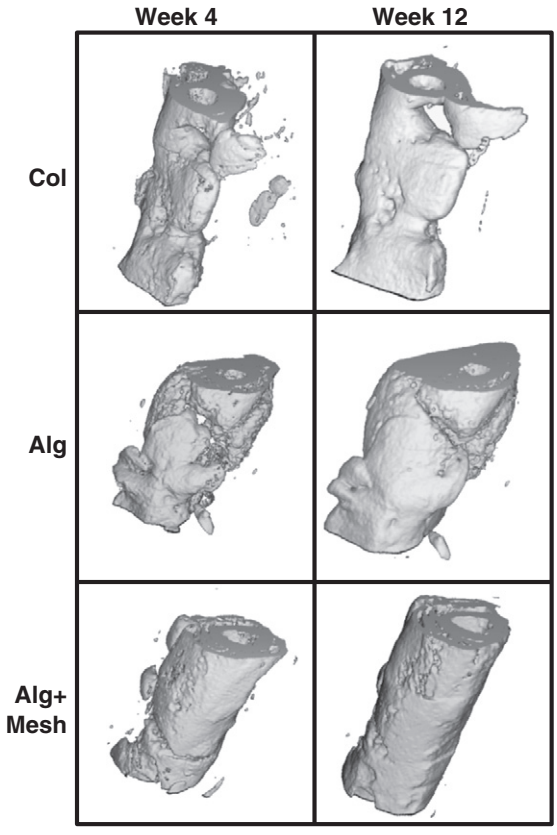

Fig. 3. Three-dimensional *in vivo* μCT images at 4 and 12 weeks. There was evidence of ample bone formation in the Col group specimens. Substantial bone formation in the Alg group occurred outside the defect. Alg + Mesh specimens, containing a nanofiber mesh tube, demonstrated continuous cylindrical bone distribution within the defect. $n = 9$–10 defects per group.

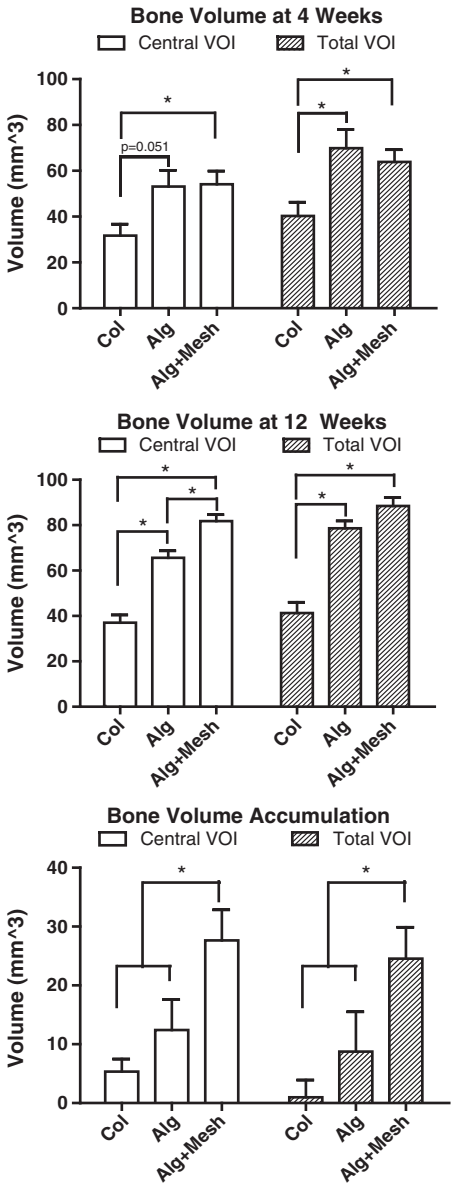

Fig. 4. Quantitative μCT analysis of new bone volume. The Alg and Alg + Mesh groups had significantly higher bone formation than the Col group at both time points in the total VOI. At 12 weeks, the Alg + Mesh group possessed more bone in the central VOI region than the Alg group, consistent with the three-dimensional images. The Alg + Mesh group also saw the largest increase in the bone volume between 4 and 12 weeks. * indicates significantly different ($p < 0.05$). $n = 9$–10 defects per group. Results are presented as mean ± SEM.

within the centeral VOI (Fig. 4). At 12 weeks, bone volume in both hydrogel groups remained significantly higher than the Col group in both total and central VOI. Moreover, a difference between the hydrogel groups was observed within the central VOI only, indicating that the hybrid alginate/mesh delivery system supported the highest level of bone ingrowth into the defect region. The change in bone volume between 4 and 12 weeks was also calculated for each specimen (Fig. 4). This analysis demonstrated that the hybrid Alg + Mesh specimens had the largest accumulation of mineralized tissue between the two time points.

Mean density and connectivity density of the newly formed bone were also evaluated from the μCT scans (Fig. 5A and B). The results indicate that the mean bone density in the Alg + Mesh specimens was significantly lower than those in the other two groups, at both time points and in both VOIs. Note that the density obtained from the μCT is

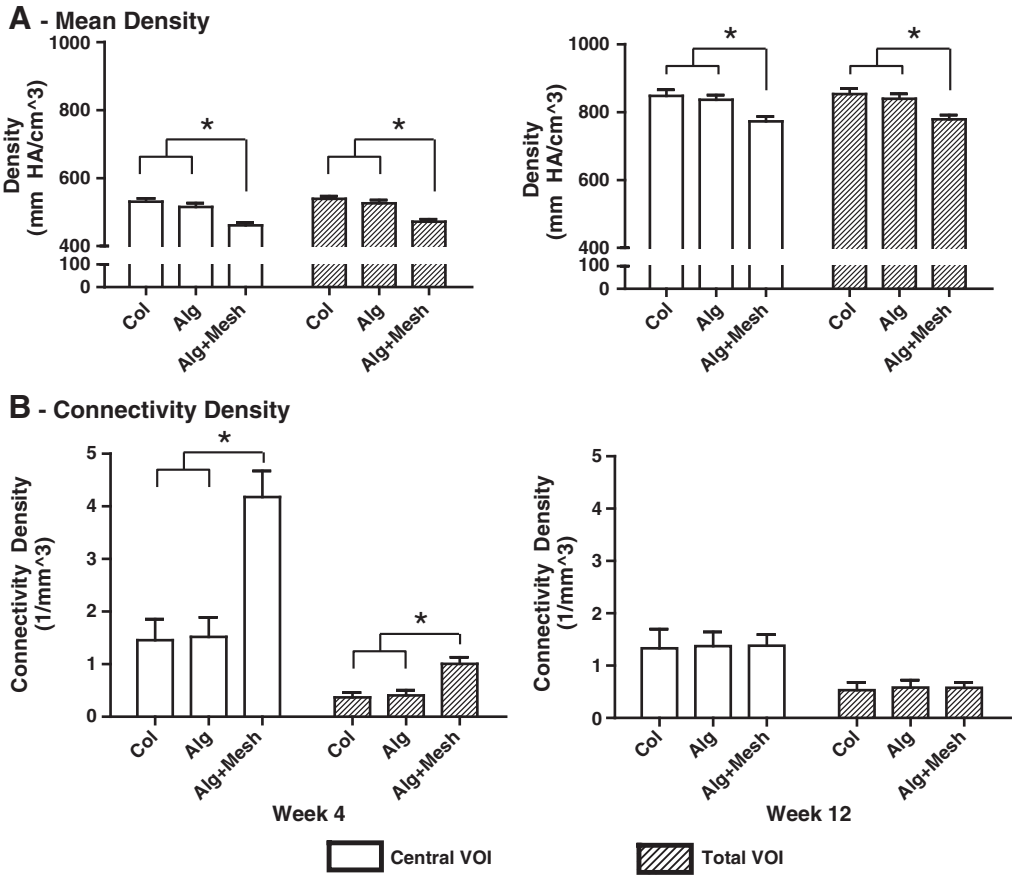

Fig. 5. Mean density (A) and connectivity density (B) of newly formed bone, obtained from μCT analysis. Mean density was significantly lower in the Alg + Mesh group compared to the other two groups, at both time points and in both VOIs. Connectivity density was the highest in the Alg + Mesh specimens at week 4, but no differences were observed at week 12. * indicates significantly different ($p<0.05$). $n=9$–10 defects per group. Results are presented as mean ± SEM.

the tissue-level bone density that is dependent on the mineralizing tissue only and not the apparent bone density that is a function of both local bone density and volume. There was more than a 50% increase in the density of all groups between 4 and 12 weeks, indicating maturation of the mineralized tissue. Connectivity density is a parameter used to analyze trabecular bone, and is a measure of the relative ratio of trabecular connections and struts in a unit volume [32]. Though regenerating bone does not consist of mature trabeculae, the direct mineralization induced by BMPs is initiated at discrete locations, which then develop connections as the mineralization progresses [33]. The connectivity obtained from the μCT analysis of regenerating bone is a measure of these connections. The connectivity density in the Alg + Mesh group was significantly higher than the other two groups in both the VOIs at 4 weeks, though there were no differences at 12 weeks. Finally, it was observed that the newly formed bone in the central VOI displayed higher connectivity density than that contained in the total VOI.

Biomechanical properties

Biomechanical properties of the regenerated femurs were obtained from torsional testing at 12 weeks. The maximum torque was 58% higher for the Alg + Mesh specimens, compared to Col specimens (Fig. 6). In addition, the torsional stiffness and work to failure of the Alg + Mesh specimens were significantly higher than those in the Col group by 58% and 102%, respectively. There were no significant differences in the failure angle between the groups. Interestingly, there were no differences in the biomechanical properties between the Col and Alg groups. There were no significant differences in any of the biomechanical properties between the Alg and Alg + Mesh groups; however the mean values of all parameters were higher for the Alg + Mesh specimens.

Histological analysis

Five micron mid-sagittal sections of the regenerated femora were stained with H&E and analyzed at 12 weeks. Consistent with the radiographs and μCT images, the histological images revealed differences in the amount, pattern and distribution of de novo bone formation between groups. The defects in the alginate groups (Alg and Alg + Mesh) appeared to possess higher amounts of well-integrated bone than the collagen sponge group (Col), which displayed a more dispersed pattern (Fig. 7). Osteocytes were seen embedded in the mineralized matrix in all groups, indicating the physiologic nature of the deposited mineral. Numerous small pockets of residual alginate surrounded by bony tissue were observed in the two alginate groups. In contrast to the substantial bone formation external to the defect region in the Alg group, the nanofiber mesh tube spatially constrained the bone regeneration in the Alg + Mesh group. The PCL nanofiber mesh was partially degraded due to the GMA processing steps, but was still observed to be present surrounding the defect.

Discussion

This study quantitatively compared the bone repair efficacy of a hybrid BMP delivery system to that of the current clinical standard of collagen delivery. Compared to delivery from a collagen matrix, rhBMP-2 delivered at the same dose via alginate hydrogel resulted in

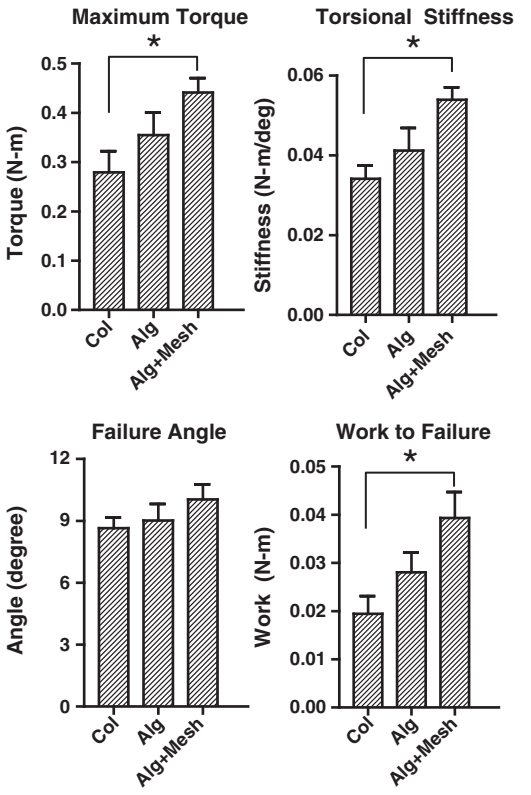

Fig. 6. Biomechanical properties of regenerated femurs obtained at 12 weeks by torsional testing. The Alg + Mesh specimens demonstrated higher maximum torque, torsional stiffness and work to failure than those in the Col group. No significant differences were observed in other comparisons. * indicates significantly different ($p<0.05$). $n=7$–8 defects per group. Results are presented as mean ± SEM.

enhanced bone formation as early as 4 weeks. The addition of a perforated nanofiber mesh to spatially retain the alginate resulted in an increased mineral accumulation between 4 and 12 weeks and led to improved bone localization in the defect region at 12 weeks. Finally, biomechanical function was significantly improved following treatment with the hybrid alginate/nanofiber mesh delivery system, compared to collagen delivery.

The amount of *de novo* bone formation in the segmental defects was influenced by the method of BMP delivery. After 2 weeks post-surgery, defects that received rhBMP-2 via collagen sponge appeared to possess higher amounts of mineral deposition compared to alginate delivery. However, by 4 weeks, the alginate groups demonstrated higher bone volume than the collagen group, and this trend continued through week 12, indicating that the kinetics of bone repair is dependent on the delivery system. These results suggest that whereas rhBMP-2 diffuses rapidly from the collagen sponge, the alginate hydrogel is able to improve long-term protein retention at the defect site. The attachment of BMP to collagen has been found to be mainly dependent on non-covalent bonding, which results in rapid and unpredictable protein release *in vivo* [34]. It has been reported that there is a significant initial burst release with collagen delivery, with less than 5% of BMP retained within the collagen sponge by 2 weeks *in vivo* [35,36]. This suggests that collagen sponge may have limited efficacy as a sustained delivery vehicle. On the other hand, the ability of alginate hydrogel to provide long-term delivery of proteins has been reported in a number of studies [37–39]. In a previous *in vitro* study, we conservatively estimated that 10% of the encapsulated rhBMP-2 remained attached to alginate after 3 weeks [28], suggesting that the protein binds to the alginate matrix and may be available to invading progenitor cells at later time points. However, further studies that directly track *in vivo* protein retention are needed to elucidate the mechanism behind the differences between the two delivery methods.

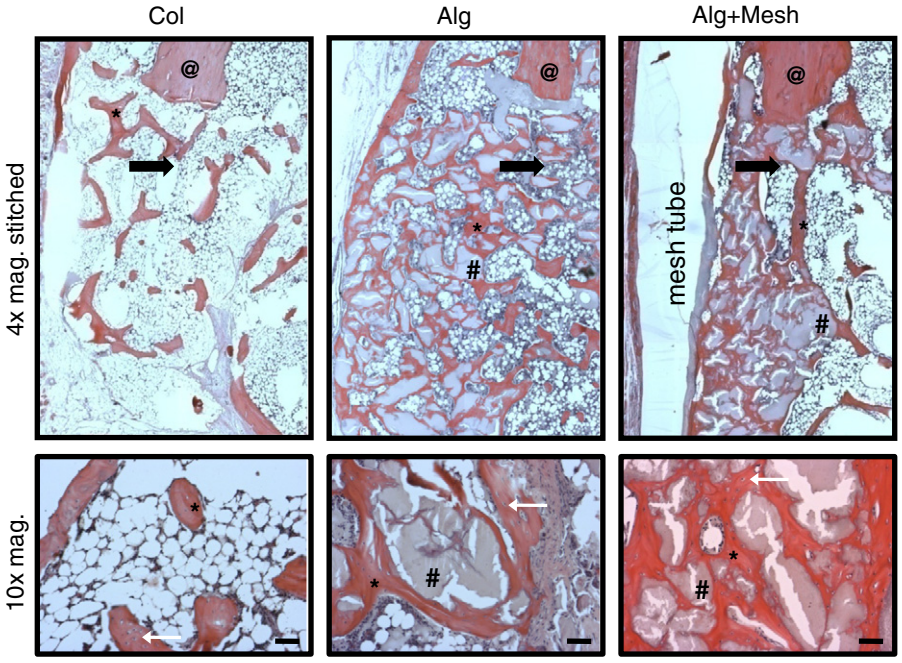

Fig. 7. Histological analysis at 12 weeks (4× and 10× magnification). H&E staining revealed improved bone regeneration in the two alginate groups, despite presence of residual alginate. The mesh tube in the Alg + Mesh group was able to constrain bone formation within the defect region. The black arrows are at located at the edges of the defects and point towards the center of the defects. The higher magnification images reveal osteocytes embedded in the newly formed bone (located with white arrows). Scale bars are 200 μm. @—native bone end; *—regenerated bone; #—residual alginate. $n=2$ defects per group.

The presence of a spatial constraint in the form of the nanofiber mesh tube influenced the bone regeneration process. Addition of the mesh tube to the alginate hydrogel did not enhance overall bone formation that was seen in the total VOI at 12 weeks, but resulted in a distinct localization of bone formation inside the defect. In contrast, substantial bone formation occurred outside the defect region in the alginate alone group, which implies hydrogel fragmentation and/or protein leakage to the surrounding area. Analysis of the central VOI, which excluded this irregular bone formation, revealed that presence of the nanofiber mesh tube did indeed improve bone formation within the defect region. The Alg + Mesh specimens also demonstrated the highest connectivity density early on, indicating a more interconnected bone structure, perhaps due to the containment provided by the mesh tube. There were no differences in connectivity density at 12 weeks, and the values were uniformly low. This could be due to the fact that as the defect fills with bony tissue, the initial finely trabeculated bone morphology is consolidated to larger structures with fewer connections through the normal remodeling process.

In addition to improvements in mineral distribution, the hybrid delivery extended the phase of bone formation resulting in the highest mineral accumulation between 4 and 12 weeks. These suggest that the nanofiber mesh tube in the hybrid system provides spatial control of bone formation by containing the alginate and/or exogenous growth factor within the defect region. It is possible that the nanofiber mesh tube slows the protein diffusion from the implant by binding the protein through nonspecific interactions. Alternatively, the nanofiber mesh tube may function by constraining and thereby compacting the BMP-containing hydrogel, which could improve the local confinement at later time points. In contrast to the higher bone volume in the Alg + Mesh group, this group displayed the lowest local bone tissue density. This apparent contradiction can be explained by the fact that sustained mineral deposition in the hybrid group results in a greater proportion of immature, lower density tissue, which reduces the overall tissue density averaged over the defect volume. It should be noted that the reported bone density is the tissue-level bone density that is dependent only on the actual local tissue.

A few recent studies have highlighted the advantage of utilizing a tubular scaffold in retaining biologic factors at the defect site [40–42]. For instance, Giardino et al. demonstrated that when a 400 μm thick poly-DL-lactide tube was utilized to constrain dimineralized bone matrix and bone marrow stromal cells within segmental defects, it led to a significant increase in the thickness of newly-formed bone [41]. A recent clinical procedure that creates a fibrous sheath to localize osteogenic factors also illustrates the benefits of a delivery system that features a retention mechanism [43,44]. In this two-stage procedure, a non-degradable polymethylmethacrylate spacer is first placed in the defect following limb stabilization. The spacer is removed after several months, and the encapsulating fibrous membrane is filled with autologous bone graft. The hybrid alginate/nanofiber mesh system provides a similar “container” effect without the need for a second surgery.

The biomechanical properties of the regenerated femurs were improved by rhBMP-2 delivery via the hybrid system. Maximum torque, torsional stiffness and work to failure were significantly higher in the Alg + Mesh specimens, when compared to those in the Col group. This indicates that the higher bone volume in the Alg + Mesh group compensated for the lower mineral density in contributing to the superior biomechanical properties. It should be noted that the torsional properties of the regenerated femurs in the Alg + Mesh group exceeded those of age-matched intact femurs determined previously [28]. There were no significant differences in the biomechanical properties between the two alginate groups. This suggests that although irregular, the bony tissue outside the defect in the Alg group contributed somewhat to the overall mechanical properties.

The delivery of BMPs for large bone defect repair has been tested in a number of animal models, including the rat model; however high protein doses are typically required [45–48]. For instance, Cuomo et al. reported that delivery of 10 μg rhBMP-2 (double the dose used in this study) resulted in bony bridging of a less challenging 6 mm rat segmental defect [48]. The 5 μg dose we utilized in this study is low compared to that used in similar rat models [46–48], suggesting that the lower BMP doses may be efficaciously delivered in the alginate/nanofiber mesh system. It should be noted that, compared to the clinical rhBMP-2 dosage of 1.5 mg/mL, the rhBMP-2 concentration we delivered in all groups was 33.33 μg/mL, which is 45 times less. Furthermore, when normalized by body weight, the amount of rhBMP-2 we delivered comes out to 0.020 mg/kg (rhBMP-2 weight/body weight) compared to the clinical dosage of 0.136 mg/kg (assuming an average body weight of 88 kg for a human patient, based on [15]). Part of this 7× reduction in required rhBMP-2 may be explained by the fact that sensitivity of human bone marrow stromal cells to BMP is lower compared to cells derived from rats [49,50]. Nonetheless, given the superior results obtained by delivering rhBMP-2 in the alginate/nanofiber mesh system compared to collagen in the same animal model, this study suggests that some of the benefits may translate to human patients.

The results of this study demonstrated that the spatiotemporal delivery of rhBMP-2 via the hybrid alginate/nanofiber mesh system resulted in improved bone repair compared to delivery on a collagen sponge. Our hypothesis is that the hybrid system is able to enhance bone regeneration by prolonging the retention of rhBMP-2 in the defect region. By maintaining sustained and localized availability of rhBMP-2, the hybrid system may result in improved clinical outcomes at a lower dose, which could reduce the cost and complications associated with collagen delivery. In conclusion, this study provides promising evidence in a challenging small animal model that spatiotemporal protein delivery strategies enhance the therapeutic efficacy of BMP in the repair of large bone defects.

Acknowledgments

This study was supported with funding from NIH R37 DE013033, NIH R01 AR051336, the Armed Forces Institute for Regenerative Medicine (AFIRM), and the Center for Advanced Engineering and Soldier Survivability (CABSS). The authors would like to thank Angela Lin and Dr. Laura O'Farrell for assistance with μCT analysis and animal welfare, respectively. We gratefully acknowledge the assistance provided by Eric Deutsch, Dr. Tamim Diab, Chris Dosier, Dr. Mela Johnson, Jessica O'Neal, Hazel Stevens, Dr. Megan Oest, Brent Uhrig, Jason Wang and Dr. Liqin Xie during surgeries.

References

[1] Cypher TJ, Grossman JP. Biological principles of bone graft healing. J Foot Ankle Surg 1996;35:413–7.
[2] Arrington ED, Smith WJ, Chambers HG, Bucknell AL, Davino NA. Complications of iliac crest bone graft harvesting. Clin Orthop Relat Res 1996;329:300–9.
[3] Berrey Jr BH, Lord CF, Gebhardt MC, Mankin HJ. Fractures of allografts. Frequency, treatment, and end-results. J Bone Joint Surg Am 1990;72:825–33.
[4] Wheeler DL, Enneking WF. Allograft bone decreases in strength in vivo over time. Clin Orthop Relat Res 2005;435:36–42.
[5] Giannoudis PV, Dinopoulos H, Tsiridis E. Bone substitutes: an update. Injury 2005;36(Suppl 3):S20–7.
[6] Schmitt JM, Hwang K, Winn SR, Hollinger JO. Bone morphogenetic proteins: an update on basic biology and clinical relevance. J Orthop Res 1999;17:269–78.
[7] De Biase P, Capanna R. Clinical applications of BMPs. Injury 2005;36:43–6.
[8] Critchlow MA, Bland YS, Ashhurst DE. The effect of exogenous transforming growth factor-beta 2 on healing fractures in the rabbit. Bone 1995;16:521–7.
[9] Street J, Bao M, deGuzman L, Bunting S, Peale Jr FV, Ferrara N, et al. Vascular endothelial growth factor stimulates bone repair by promoting angiogenesis and bone turnover. Proc Natl Acad Sci USA 2002;99:9656–61.
[10] Reddi AH. Role of morphogenetic proteins in skeletal tissue engineering and regeneration. Nat Biotechnol 1998;16:247–52.

[11] Lieberman AD JR, Einhorn TA. The role of growth factors in the repair of bone: biology and clinical applications. The Journal of Bone and Joint Surgery 2002;84-A: 1032–44.
[12] Tsuji K, Bandyopadhyay A, Harfe BD, Cox K, Kakar S, Gerstenfeld L, et al. BMP2 activity, although dispensable for bone formation, is required for the initiation of fracture healing. Nat Genet 2006;38:1424–9.
[13] Wozney JM, Rosen V. Bone morphogenetic protein and bone morphogenetic protein gene family in bone formation and repair. Clin Orthop Relat Res 1998;346: 26–37.
[14] Lind M, Eriksen EF, Bunger C. Bone morphogenetic protein-2 but not bone morphogenetic protein-4 and -6 stimulates chemotactic migration of human osteoblasts, human marrow osteoblasts, and U2-OS cells. Bone 1996;18:53–7.
[15] Swiontkowski MF, Aro HT, Donell S, Esterhai JL, Goulet J, Jones A, et al. Recombinant human bone morphogenetic protein-2 in open tibial fractures. A subgroup analysis of data combined from two prospective randomized studies. J Bone Joint Surg Am 2006;88:1258–65.
[16] Chen RR, Mooney DJ. Polymeric growth factor delivery strategies for tissue engineering. Pharm Res 2003;20:1103–12.
[17] Rose FR, Hou Q, Oreffo RO. Delivery systems for bone growth factors—the new players in skeletal regeneration. J Pharm Pharmacol 2004;56:415–27.
[18] Garrison KR, Donell S, Ryder J, Shemilt I, Mugford M, Harvey I, et al. Clinical effectiveness and cost-effectiveness of bone morphogenetic proteins in the non-healing of fractures and spinal fusion: a systematic review. Health Technol Assess 2007;11:1–150.
[19] Umulis D, O'Connor MB, Blair SS. The extracellular regulation of bone morphogenetic protein signaling. Development 2009;136:3715–28.
[20] Cahill KS, Chi JH, Day A, Claus EB. Prevalence, complications, and hospital charges associated with use of bone-morphogenetic proteins in spinal fusion procedures. JAMA 2009;302:58–66.
[21] Benglis D, Wang MY, Levi AD. A comprehensive review of the safety profile of bone morphogenetic protein in spine surgery. Neurosurgery 2008;62:ONS423–31.
[22] Shields LB, Raque GH, Glassman SD, Campbell M, Vitaz T, Harpring J, et al. Adverse effects associated with high-dose recombinant human bone morphogenetic protein-2 use in anterior cervical spine fusion. Spine (Phila Pa 1976) 2006;31: 542–7.
[23] Dahabreh Z, Calori GM, Kanakaris NK, Nikolaou VS, Giannoudis PV. A cost analysis of treatment of tibial fracture nonunion by bone grafting or bone morphogenetic protein-7. Int Orthop 2008.
[24] Garrison KR, Donell S, Ryder J, Shemilt I, Mugford M, Harvey I, et al. Clinical effectiveness and cost-effectiveness of bone morphogenetic proteins in the non-healing of fractures and spinal fusion: a systematic review. Health Technol Assess 2007;11:1–150 iii-iv.
[25] Yamamoto M, Takahashi Y, Tabata Y. Enhanced bone regeneration at a segmental bone defect by controlled release of bone morphogenetic protein-2 from a biodegradable hydrogel. Tissue Eng 2006;12:1305–11.
[26] Johnson MR, Lee HJ, Bellamkonda RV, Guldberg RE. Sustained release of BMP-2 in a lipid-based microtube vehicle. Acta Biomater 2009;5:23–8.
[27] Lutolf MP, Weber FE, Schmoekel HG, Schense JC, Kohler T, Muller R, et al. Repair of bone defects using synthetic mimetics of collagenous extracellular matrices. Nat Biotechnol 2003;21:513–8.
[28] Kolambkar YM, Dupont KM, Boerckel JD, Huebsch N, Mooney DJ, Hutmacher DW, et al. An alginate-based hybrid system for growth factor delivery in the functional repair of large bone defects. Biomaterials 2011;32:65–74.
[29] Rowley JA, Madlambayan G, Mooney DJ. Alginate hydrogels as synthetic extracellular matrix materials. Biomaterials 1999;20:45–53.
[30] Kong H-J, Lee KY, Mooney DJ. Decoupling the dependence of rheological/ mechanical properties of hydrogels from solids concentration. Polymer 2002;43: 6239–46.
[31] Oest ME, Dupont KM, Kong HJ, Mooney DJ, Guldberg RE. Quantitative assessment of scaffold and growth factor-mediated repair of critically sized bone defects. J Orthop Res 2007;25:941–50.
[32] Odgaard A, Gundersen HJ. Quantification of connectivity in cancellous bone, with special emphasis on 3-D reconstructions. Bone 1993;14:173–82.
[33] Buckwalter JA, Glimcher MJ, Cooper RR, Recker R. Bone biology. II: formation, form, modeling, remodeling, and regulation of cell function. Instr Course Lect 1996;45:387–99.
[34] Uludag H, Friess W, Williams D, Porter T, Timony G, D'Augusta D, et al. rhBMP-collagen sponges as osteoinductive devices: effects of in vitro sponge characteristics and protein pI on in vivo rhBMP pharmacokinetics. Ann N Y Acad Sci 1999;875:369–78.
[35] Winn SR, Uludag H, Hollinger JO. Carrier systems for bone morphogenetic proteins. Clin Orthop Relat Res 1999;367(Suppl):S95–S106.
[36] Uludag H, Gao T, Porter TJ, Friess W, Wozney JM. Delivery systems for BMPs: factors contributing to protein retention at an application site. J Bone Joint Surg Am 2001;83-A(Suppl 1):S128–35.
[37] Lee KY, Peters MC, Anderson KW, Mooney DJ. Controlled growth factor release from synthetic extracellular matrices. Nature 2000;408:998–1000.
[38] Silva EA, Mooney DJ. Spatiotemporal control of vascular endothelial growth factor delivery from injectable hydrogels enhances angiogenesis. J Thromb Haemost 2007;5:590–8.
[39] Simmons CA, Alsberg E, Hsiong S, Kim WJ, Mooney DJ. Dual growth factor delivery and controlled scaffold degradation enhance in vivo bone formation by transplanted bone marrow stromal cells. Bone 2004;35:562–9.
[40] Gugala Z, Gogolewski S. Regeneration of segmental diaphyseal defects in sheep tibiae using resorbable polymeric membranes: a preliminary study. J Orthop Trauma 1999;13:187–95.
[41] Giardino R, Nicoli Aldini N, Fini M, Tanzi MC, Fare S, Draghi L, et al. Bioabsorbable scaffold for in situ bone regeneration. Biomed Pharmacother 2006;60:386–92.
[42] Lindsey RW, Gugala Z, Milne E, Sun M, Gannon FH, Latta LL. The efficacy of cylindrical titanium mesh cage for the reconstruction of a critical-size canine segmental femoral diaphyseal defect. J Orthop Res 2006;24:1438–53.
[43] Masquelet AC. Muscle reconstruction in reconstructive surgery: soft tissue repair and long bone reconstruction. Langenbecks Arch Surg 2003;388:344–6.
[44] Biau DJ, Pannier S, Masquelet AC, Glorion C. Case report: reconstruction of a 16-cm diaphyseal defect after Ewing's resection in a child. Clin Orthop Relat Res 2009;467:572–7.
[45] Pluhar GE, Manley PA, Heiner JP, Vanderby Jr R, Seeherman HJ, Markel MD. The effect of recombinant human bone morphogenetic protein-2 on femoral reconstruction with an intercalary allograft in a dog model. J Orthop Res 2001;19:308–17.
[46] Chen X, Schmidt AH, Mahjouri S, Polly Jr DW, Lew WD. Union of a chronically infected internally stabilized segmental defect in the rat femur after debridement and application of rhBMP-2 and systemic antibiotic. J Orthop Trauma 2007;21: 693–700.
[47] Yasko AW, Lane JM, Fellinger EJ, Rosen V, Wozney JM, Wang EA. The healing of segmental bone defects, induced by recombinant human bone morphogenetic protein (rhBMP-2). A radiographic, histological, and biomechanical study in rats. J Bone Joint Surg Am 1992;74:659–70.
[48] Cuomo AV, Virk M, Petrigliano F, Morgan EF, Lieberman JR. Mesenchymal stem cell concentration and bone repair: potential pitfalls from bench to bedside. J Bone Joint Surg Am 2009;91:1073–83.
[49] Osyczka AM, Diefenderfer DL, Bhargave G, Leboy PS. Different effects of BMP-2 on marrow stromal cells from human and rat bone. Cells Tissues Organs 2004;176: 109–19.
[50] Diefenderfer DL, Osyczka AM, Reilly GC, Leboy PS. BMP responsiveness in human mesenchymal stem cells. Connect Tissue Res 2003;44(Suppl 1):305–11.